

Article

# Non-Invasive Spectral Phenotyping Methods can Improve and Accelerate *Cercospora* Disease Scoring in Sugar Beet Breeding

Marcus Jansen <sup>1</sup>, Sergej Bergsträsser <sup>1</sup>, Simone Schmittgen <sup>1</sup>, Mark Müller-Linow <sup>1</sup> and Uwe Rascher <sup>1,2,\*</sup>

<sup>1</sup> Forschungszentrum Jülich GmbH, Institut für Bio- und Geowissenschaften, IBG-2, Pflanzenwissenschaften, Wilhelm-Johnen-Straße, Jülich 52425, Germany; E-Mails: m.jansen@fz-juelich.de (M.J.); s.bergstraesser@fz-juelich.de (S.B.); si.schmittgen@fz-juelich.de (S.S.); m.mueller-linow@fz-juelich.de (M.M.-L.)

<sup>2</sup> Rheinische Friedrich-Wilhelms-Universität Bonn, Regina-Pacis-Weg 3, Bonn 53113, Germany

\* Author to whom correspondence should be addressed; E-Mail: u.rascher@fz-juelich.de; Tel.: +49-2461612638; Fax: +49-2461612492.

Received: 27 March 2014; in revised form: 25 April 2014 / Accepted: 29 April 2014 /

Published: 8 May 2014

---

**Abstract:** Breeding for *Cercospora* resistant sugar beet cultivars requires field experiments for testing resistance levels of candidate genotypes in conditions that are close to agricultural cultivation. Non-invasive spectral phenotyping methods can support and accelerate resistance rating and thereby speed up breeding process. In a case study, experimental field plots with strongly infected beet genotypes of different resistance levels were measured with two different spectrometers. Vegetation indices were calculated from measured wavelength signature to determine leaf physiological status, e.g., greenness with the Normalized Differenced Vegetation Index (NDVI), leaf water content with the Leaf Water Index (LWI) and *Cercospora* disease severity with the *Cercospora* Leaf Spot Index (CLSI). Indices values correlated significantly with visually scored disease severity, thus connecting the classical breeders' scoring approach with advanced non-invasive technology.

**Keywords:** phenotyping; vegetation index; disease scoring; *Cercospora beticola*; resistance breeding

---

## 1. Introduction

Sugar beets (*Beta vulgaris* spp. *vulgaris*) are frequently infested by the fungal pathogen *Cercospora beticola* that occurs in moderate climatic areas and causes yield loss between 40% and 100% [1,2]. Plant protection against *Cercospora* leaf spot (CLS) usually includes crop rotation, fungicide application, and the use of resistant cultivars [1]. Resistant cultivars frequently are low yielding when infection is absent [3] and breeding efforts aim at novel genotypes with stable yield at infected as well as infection-free sites. Breeding for CLS resistant cultivars requires field experiments for testing resistance levels of candidate genotypes in conditions that are close to agricultural cultivation. In such experiments, disease progression generally is monitored via scoring by experienced breeding personnel.

Non-invasive spectral phenotyping methods [4,5] can support disease scoring by providing information on the plant status [6]. This in turn has the potential to accelerate resistance rating and speed up the breeding process. Optical measurements possess the advantage of objective and precise scoring [7]. Remote sensing signals can be collected by ground level and airborne measurements [8] based on the detection of reflected light or chlorophyll fluorescence of the vegetation canopy. The reflected light from the leaf surface is influenced by surface properties and physiological features, for example: trichomes, epicuticular waxes and leaf pigment composition [9,10]. Pigments such as chlorophyll, anthocyanins and carotenoids absorb the incoming light in the visible region (400–700 nm), whereas light of the near-infrared region (700–1200 nm) is absorbed by water, proteins and other carbohydrate molecules (e.g., lignin). Differences in the reflectance signature can be referred to changes in the pigment composition, surface morphology and plant density on the field [7]. Hyperspectral sensors give insight into the quality of the reflected or transmitted light. On the one hand, measuring devices can integrate the spectral signature of an area of interest (point spectrometers), on the other hand they can image the spectral signature of each image pixel leading to a three dimensional cube with wavelength as Z-component (hyperspectral imaging) [11]. Multispectral sensors detect specific parts of electromagnetic radiation, so called wideband channels, instead of the whole spectrum. Specific wavelength of the signature can be taken into account to calculate vegetation indices giving information about plant properties [10,12], e.g., the Normalized Differenced Vegetation Index (NDVI), the Leaf Water Index (LWI) and the *Cercospora* Leaf Spot Index (CLSI) [13]. Multiple indices are in use (Table 1) giving information about e.g., water content (Water Index–WI; Normalized Difference Water Index–NDWI<sub>1240/1640</sub>) photosynthetic activity (Photochemical Reflectance Index–PRI), chlorophyll content (Pigment Specific Simple ratio–PSSRa/b; Pigment Specific Normalized Difference–PSNDa), carotenoids (Structure Insensitive Pigment Index–SIPI; Carotenoids Reflectance Index–CRI<sub>1</sub>) or anthocyanins (Anthocyanin Reflectance Index–ARI<sub>1</sub>). Each vegetation index is calculated out of two or three spectral bands.

**Table 1.** Vegetation indices calculated out of two or three wavelengths indicating traits related to physiological status of leaves.

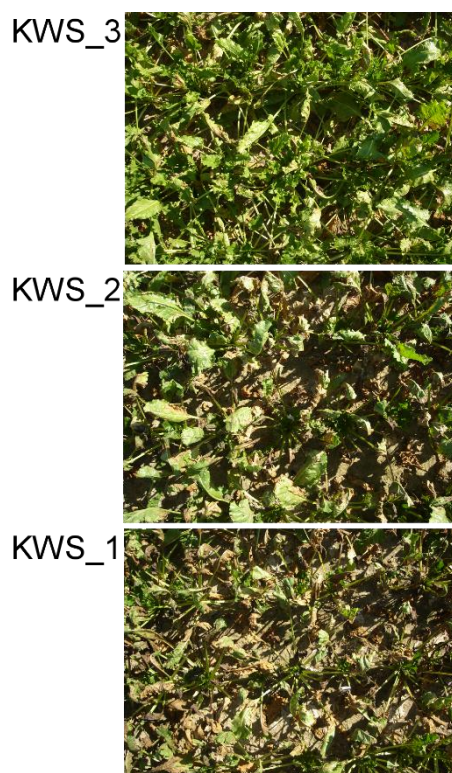
Index	Formula	Indicator	Reference
NDVI, normalized difference vegetation index	$(R800 - R670) \times (R800 + R670)^{-1}$	Biomass, leaf area	[14]
PRI, photochemical reflectance index	$(R531 - R570) \times (R531 + R570)^{-1}$	Estimates xanthophyll epoxidation as a measure of photosynthetic activity	[15]
SIPI, structure insensitive pigment index	$(R800 - R455) \times (R800 + R680)^{-1}$	Carotenoid/Chlorophyll a ratio	[16]
PSSRa, pigment specific simple ratio	$R800 \times R680^{-1}$	Chlorophyll a	[17]
PSSRb	$R800 \times R635^{-1}$	Chlorophyll b	[17]
WI, water index	$R900 \times R970^{-1}$	Water content	[18]
CRI <sub>1</sub> , carotenoids reflectance index	$R510^{-1} + R550^{-1}$	Carotenoid content	[19]
ARI <sub>1</sub> , anthocyanin reflectance index	$R550^{-1} + R700^{-1}$	Anthocyanin content	[20]
PSNDa, pigment specific normalized difference	$(R800 - R680) \times (R800 + R680)^{-1}$	Chlorophyll a	[17]
NDWI <sub>1240</sub> , normalized difference water index	$(R980 - R1240) \times (R980 + R1240)^{-1}$	Water content	[21]
NDWI <sub>1640</sub>	$(R858 - R1640) \times (R858 + R1640)^{-1}$	Water content	[22]
LWI, leaf water index	$R1300 \times R1450^{-1}$	Water content	[23]
CLSI, <i>Cercospora</i> leaf spot index	$(R698 - R570) \times (R698 + R570)^{-1} + R734$	<i>Cercospora</i> leaf spot classification	[13]

In a case study, we carried out visual scoring and non-invasive phenotyping on trial fields with sugar beet breeding genotypes with different levels of CLS disease severity. The fungus evokes changes in leaf properties that differ according to developmental stages and disease severity [24]. Such changes result in modification of spectral signatures and thereby lead to alterations in index values. Beyond detecting the presence of a certain change, it is a challenging issue to assign this change to a biological response of the plants. Connecting dynamics in spectral properties with biological events allows the use of spectral data for monitoring plant status. In order to achieve this goal, we correlated measured data with biological reactions. In our study, we acquired spectral data using a FieldSpec point spectrometer and a Tetracam Agriculture Digital Camera and compared these data with visual disease scoring.

## 2. Results and Discussion

Sugar beet plants of three genotypes, KWS\_1 (high susceptibility to CLS), KWS\_2 (intermediate susceptibility to CLS), KWS\_3 (low susceptibility to CLS) growing in plots at the Plattling (southern Germany) trial field were visually scored for CLS disease severity using the KWS scale scoring protocol [1]. Highly susceptible KWS\_1 plants reached an average disease score of 9, meaning that there was severe leaf destruction. Plants of genotype KWS\_2 were scored at 7.5 and the KWS\_3, the genotype with the lowest susceptibility, had an average score of 5, corresponding to minor leaf damage (representative photos in Figure 1).

**Figure 1.** Photographs of representative plants in plots planted with genotypes KWS\_3 (low susceptibility, disease score 5), KWS\_2 (intermediate susceptibility, disease score 7.5), and KWS\_1 (high susceptibility, disease score 9) at Plattling experimental field site.



In the same plots, plants were measured with non-invasive spectral devices. FieldSpec, a hyperspectral device acquired reflectance data in a broad range of wavelengths when positioned above canopy level. Tetracam, a multispectral camera, captured images of the plants comprising spectral information in green, red, and NIR range. Infection-free plants (score = 1) were measured with both instruments, too. Spectral data out of both instruments were used for calculation of vegetation indices describing physiological properties of the canopy [4].

### *2.1. Tetracam Allowed Quantitative Spectral Imaging of Diseased Vegetation*

Multispectral Tetracam images showed color-coded images of the vegetation, whereas colors referred to NDVI data calculated out of spectral information (Figure 2A). NDVI as such serves as an indicator for green vegetation. In images, ratio of pixels with  $\text{NDVI} \geq 0.1$  referred to vegetation whereas pixels with  $\text{NDVI} < 0.1$  referred to soil background. Using the ratios we were able to distinguish between different degrees of canopy destruction by CLS disease progression on plots of genotypes KWS\_1, KWS\_2, and KWS\_3 (Figure 2A). Fitting a cubic regression line through the data points shows that NDVI pixel ratios correlate with disease score values. In turn, there is potential for calculating disease score values from NDVI images. However, this holds true only when there are no other factors causing leaf damage. Therefore, the method seems applicable when measuring inoculated plants in a test site, but not for measurements in agriculture where source of leaf damage is unknown. Nevertheless, even when source of damage is not known, pixel ratios from NDVI images may be indicative of general plant status. A potential drawback of using Tetracam images for NDVI estimation is that some pixels may be classified as vegetation although they belong to the soil background as visible on the pictures. In conclusion, Tetracam allows an overview on vegetation damage, but does not allow highly accurate measurements of disease severity because of limited spectral information.

### *2.2. FieldSpec Hyperspectral Data Enabled Assessment of Multiple Vegetation Indices*

Hyperspectral data measured with a FieldSpec instrument does not contain image information, but has a much higher spectral resolution than Tetracam images. Spectral signatures of measured plots contain a broad range of spectral information (350 nm to 2500 nm) giving the chance of calculating multiple vegetation indices using selected wavelengths, e.g., NDVI, PRI, CLSI, ARI, SIPI, PSSRa, PSSRb, WI, PSNDa,  $\text{NDWI}_{1240}$ ,  $\text{NDWI}_{1640}$ , and LWI.

In a first step, we conducted a principle component analysis (PCA) in order to evaluate whether spectral signatures discriminate between non infected plants and the infected plants of the different genotypes. We selected a subset of wavelengths in the range of 350–1350 nm and 1510–1800 nm (thereby eliminating the noise-driven regions in the spectrum) and performed the PCA with the averaged wavelength-specific reflection values (Figure 3). Non-infected plants clustered separately from infected ones. Among these, genotype KWS\_3 exhibiting low infestation (disease score 5) separated from KWS\_2 and KWS\_1. The latter genotypes also clustered, but displayed an overlapping region. This might be due to a certain ratio of open soil between strongly infested leaves and the grey to brown color of the leaf spots that shares similarity to soil color.

**Figure 2.** Tetracam images of *Cercospora* Leaf Spot (CLS) infected sugar beets; (A) ratio of pixels with Normalized Differenced Vegetation Index (NDVI) < 1 (soil) or NDVI ≥ 1 (vegetation) for plots with sugar beet plants of genotypes KWS\_1, KWS\_2, and KWS\_3 inoculated with *Cercospora beticola* as well as disease-free plants in correlation to visual disease scoring. Regression was calculated using 2nd degree polynomial fit. Pixel ratios of the three genotypes differ significantly (\*\*\*) ANOVA,  $p < 0.001$ ) from each other; (B) representative multispectral image of infected beet plants; (C) color coded NDVI image calculated out of image (B) using Tetracam PixelWrench2.

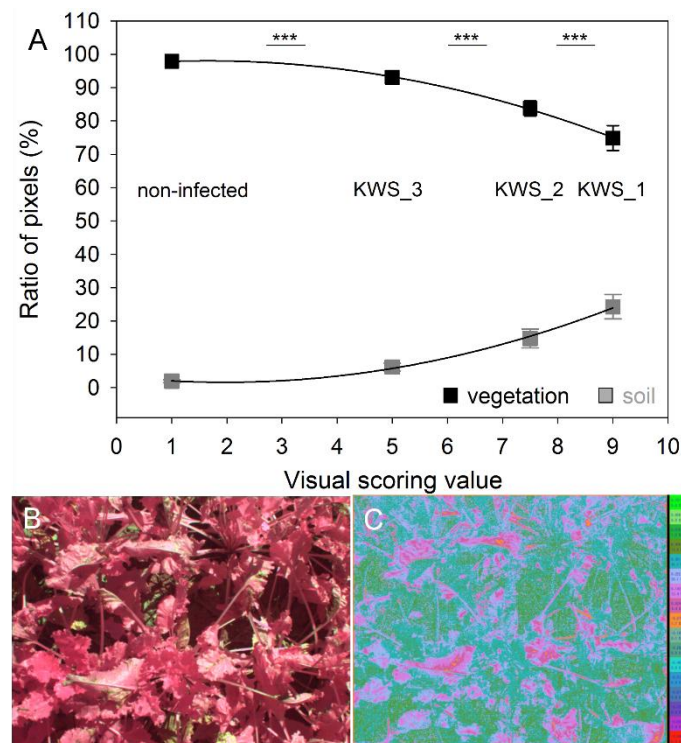
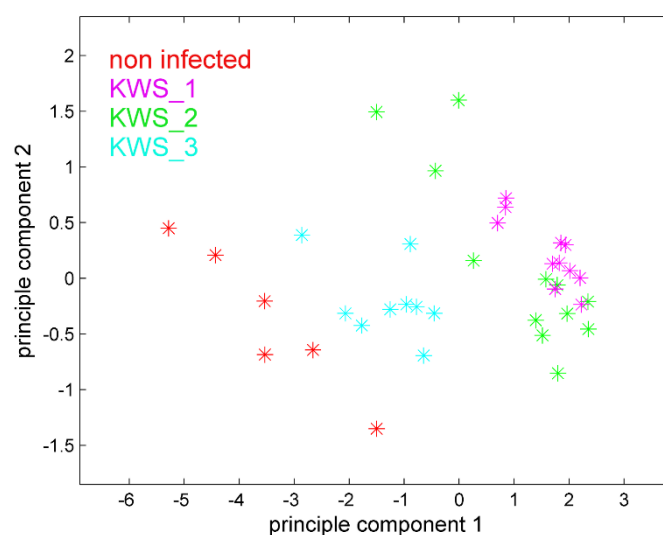


**Figure 3.** Principle component analysis of the spectral signatures from FieldSpec measurements of non-infected and infected (KWS\_1, KWS\_2, KWS\_3) sugar beets. Evaluated spectral regions comprise 350–1350 nm and 1510–1800 nm. First principal component accounts for 92% of the spectral variance (7% in the second component).



As PCA proved that data allowed discrimination between different levels of infestation, we calculated vegetation indices as a second step of data analysis. Whereas PCA uses a large spectral range for detecting differences between the genotypes, vegetation indices focus on a few specific wavelengths. Thereby, indices are reduced in information content, but this reduction might allow increased speed and throughput of measurements.

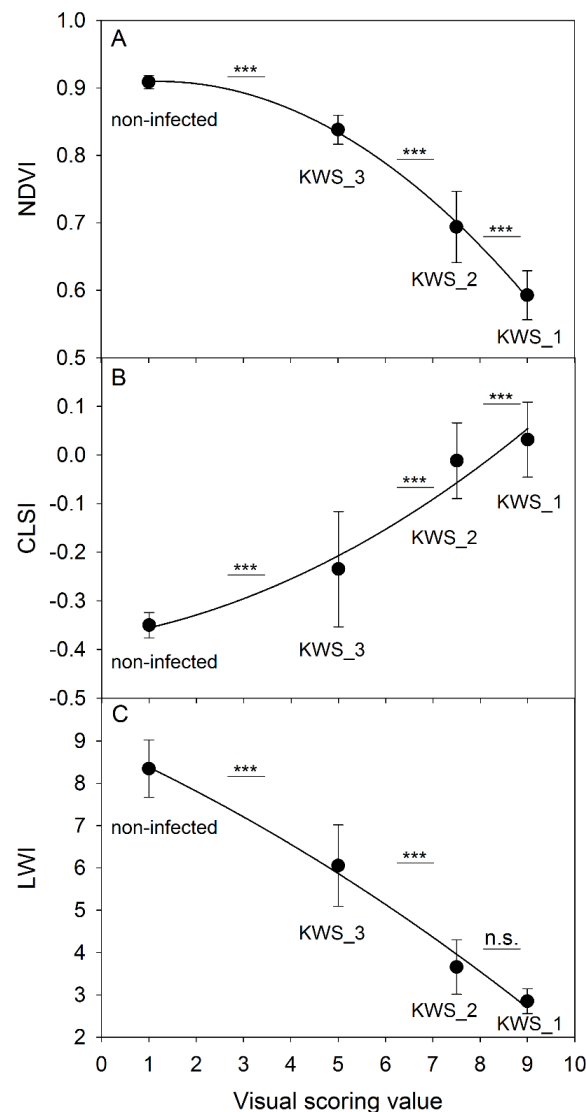
Besides NDVI, which was also used with Tetracam, we evaluated a series of indices for correlation with disease score data (Table 1). Calculating linear regressions, CRI and ARI had poor correlation with the degree of disease, but there were high correlations for NDVI, PRI, SIPI, PSSRa, PSSRb, WI, PSNDa, NDWI1240, NDWI1640, and LWI. Linear regressions, however in many cases do not fit well with the data distribution and data can be described better using 2nd degree polynomial fits (Table 1).

NDVI and LWI together with the *Cercospora*-specific CLSI were fitted with 2nd degree regressions to visual disease scores of the different genotypes (Figure 4). It could be shown that the NDVI decreased with decreasing vegetation density or increasing fungal leaf damage causing loss of green leaf area (Figure 4A). Leaf water content described by LWI changed with decreasing healthy leaf tissue because infected parts of the leaves dried out (Figure 4C). CLSI values increased with ascending disease severity (Figure 4B) which is consistent with previous reports [13].

CLS disease progression affects multiple traits that are characterized by vegetation indices. Color alterations in infected areas are due to cells becoming necrotic and senescence sets on [24]. This is accompanied by changes in pigment composition, and decrease of pigment content. Therefore pigment sensitive indices, such as PSSRa, PSSRb, ARI, and CRI proved to be responsive to different levels of disease severity.

Similar with Tetracam images, measuring aperture of FieldSpec might capture reflectance from open soil areas between the plants, too. Tetracam data proved that reflectance from soil does influence indices, in this case NDVI. Data range of NDVI acquired from open vegetation-free soil ( $<-0.12$ , FieldSpec;  $<0.36$ , Tetracam) differed clearly from data ranges of plots with infected or non-infected sugar beet plants ( $>0.53$ , FieldSpec;  $>0.58$ , Tetracam). Visible open soil between plants occurs in plots with young plants, but current measurements were done at a growth stage after canopy closure. At this stage, open soil refers either to cultivar-specific shoot architecture or any type of leaf damage or loss. In sugar beet breeding however, plants normally are selected against sparse shoot architecture. Therefore, visibility of soil between plants might be considered as indicator for improper growth, too. The soil effect might be mitigated when using CLSI, an index with specificity for *Cercospora* leaf damage. Examples show that multiple indices were responsive to increasing *Cercospora* disease severity, but not all indices enable proper discrimination at each level of disease. In particular the water content related LWI did not allow significant discrimination between plants of disease scores 7.5 (KWS\_2) and 9.0 (KWS\_1; Figure 4C), whereas other vegetation indices did so (Figures 4A,B and 2A). A possible reason might be that in both disease levels there was already high ratio of leaf desiccation due to the fungus necrotizing the tissue.

**Figure 4.** Field spec measurements. Vegetation indices were calculated out of measured spectral data and correlated with visual disease scoring values of CLS infected as well as infection-free sugar beet plants. (A) NDVI; (B) CLSI; (C) Leaf Water Index (LWI); Regressions were calculated using 2nd degree polynomial fits. Significant differences between index data of non-infected plants and diseased plants of genotypes KWS\_1, KWS\_2, and KWS\_3 are denoted with \*\*\* ANOVA,  $p < 0.001$ .



Nevertheless, regression curves indicated that vegetation indices derived from a few spectral bands can be used for estimation of disease scores. This means, that after a calibration with reference plants exhibiting different degrees of infestation, spectral data allow rating of the degree of infestation in test plots. Examples indicate that using a combination of a few indices is well suitable for this issue. A single index might be misleading in some cases, e.g., LWI when comparing KWS\_1 and KWS\_2 (Figure 4C), but high correlations (Table 2) indicate that one does not need to apply a multitude of combinations. With this knowledge, one can set up a scenario in which a dedicated spectrometer is carried across test plots using a positioning system, e.g., a conveyor or an unmanned aerial vehicle (UAV)). Thereby, it becomes possible to monitor disease progression in test plots with high temporal resolution. For practical application, a combination of high-resolution spectrometers such as FieldSpec



with imaging devices such as Tetracam can be meaningful. The advantage of spectrometers is gaining more detailed information on plant performance, e.g., biomass (NDVI), water content (LWI), photosynthetic activity (PRI), UV-protection (SIPI, CRI1, ARI1), compared to visual scoring. Imaging devices in turn give the possibility of visual reviewing the results by the operator, e.g., when measuring canopies that are not completely closed and reflectance from soil might have major influences on the measured data.

**Table 2.** Correlation of vegetation indices to visual disease scoring using 2nd degree polynomial fits.

Index	Sum of Squares	Mean of Squares	F Value	<i>p</i>
NDVI	0.73	0.36	111.76	0.00
PRI	0.01	0.01	49.27	$4.63 \times 10^{-12}$
SIPI	0.30	0.15	127.24	0.00
PSSRa	271.85	135.93	145.48	0.00
PSSRb	63.56	31.78	115.59	0.00
WI	1.30	0.65	110.08	0.00
CRI <sub>1</sub>	0.00	0.00	5.55	0.01
ARI <sub>1</sub>	0.00	0.00	7.35	0.00
PSNDa	0.78	0.39	112.78	0.00
NDWI1240	0.78	0.39	112.78	0.00
NDWI1640	1.03	0.51	124.22	0.00
LWI	5688.85	2844.43	69.73	$1.64 \times 10^{-14}$
CLSI	$5.50 \times 10^7$	$2.75 \times 10^7$	33.85	$1.07 \times 10^{-9}$

### 3. Experimental Section

Sugar beets lines—*Beta vulgaris* ssp. *vulgaris*—with different levels of susceptibility (high, KWS\_1—moderate, KWS\_2—low, KWS\_3; KWS SAAT AG, Einbeck, Germany) to *C. beticola* were grown on a trial field in Plattling, Germany, in the growth season 2012. Additionally to naturally occurring infestation in this region, dried infected plant material was used for inoculation in order to increase the infection pressure. Measurements took place in August 2012 when experimental plots were strongly infected with CLS. Visual scoring as well as measurements with the FieldSpec instrument and Tetracam were done in two individual plots per genotype with three spots within one plot (together 6 measurement points for each genotype).

The sugar beet genotypes were measured with two different spectrometers: the FieldSpec (ASD Inc., Boulder, CO, USA) with a spectral range from 350 to 2500 nm and Agriculture Digital Camera (Tetracam, Chatsworth, CA, USA) with three multispectral bands.

FieldSpec acquires an averaged spectral signature of an area of interest with a spectral resolution of 3 nm at 700 nm and 8 nm at 1400 and 2100 nm. The sampling interval by FieldSpec spectrometer is 1.4 nm in the range from 350 to 1050 nm and 2 nm in the range from 1000 to 2500 nm. Hyperspectral FieldSpec data were normalized to relative values using white reference panel

(Specralon<sup>®</sup>, Labsphere Inc., North Dutton, NH, USA) spectra. After normalization index-specific wavelengths were chosen to calculate vegetation indices (terms see Table 1).

Tetracam detects wideband channels of the green (520–600 nm), red (600–700 nm) and NIR (700–920 nm) region allowing multispectral imaging. Similar to FieldSpec, NDVI was calculated with the Tetracam data using the formula  $(\text{NIR} - \text{RED}) \times (\text{NIR} + \text{RED})^{-1}$ . Values were coded in a color scale from −1 to 1, and pixels were classified either as vegetation ( $\text{NDVI} \geq 0.1$ ) or background ( $\text{NDVI} < 0.1$ ).

#### 4. Conclusions

Our case studies show that non-invasive spectral measurements have the potential to assist and complement disease scoring in breeding plot experiments. Vegetation indices correlate with disease severity and this allows calculating disease scores from spectral data. A constraint is that in many cases established indices are not disease-specific, meaning that they can be used for quantifying an infestation or damage, e.g., caused by CLS, but in most cases they do not allow distinguishing between different types of disease. Disease identification in turn requires development of disease-specific indices or index combinations [13,25,26].

In general, the study supports the use of spectral data for disease rating purposes given that data acquisition and data analysis can be achieved with an acceptable effort. Use of automated sensor displacement systems and targeted data selection based on prior evaluation and calibration are essential for this goal. Thereby, methods have the potential of assisting, automating, and accelerating of disease scoring in the plant breeding process.

#### Acknowledgments

The authors are grateful to KWS SAAT AG (Einbeck, Germany) for allowing measurements on their experimental site at Plattling (Southern Germany) and Werner Beyer and Madlaina Peter for discussing results. Work was supported by Bundesministerium für Bildung und Forschung (BMBF, Germany) in the CROP.SENSE.net consortium.

#### Authors Contribution

Uwe Rascher designed the study; Simone Schmittgen and Sergej Bergsträsser carried out the experiments; Simone Schmittgen, Sergej Bergsträsser, Marcus Jansen, and Mark Müller-Linow analyzed the data; Simone Schmittgen, Sergej Bergsträsser, and Marcus Jansen wrote the manuscript.

#### Conflicts of Interest

The authors declare no conflict of interest.

#### References

1. Shane, W.W.; Teng, P.S. Impact of *Cercospora* leaf spot on root weight, sugar yield and purity of *Beta vulgaris*. *Plant Dis.* **1992**, *76*, 812–820.

2. Rossi, V.; Battilani, P.; Chiusa, G.; Giosue, S.; Languasco, L.; Racca, P. Components of rate-reducing resistance to *Cercospora* leaf spot in sugar beet: Conidiation length, spore yield. *J. Plant Pathol.* **2000**, *82*, 125–131.
3. Smith, G.A.; Campbell, L.G. Association between resistance to *Cercospora* and yield in commercial sugarbeet hybrids. *Plant Breed.* **1996**, *115*, 28–32.
4. Jansen, M.; Pinto, F.; Nagel, K.A.; Dusschoten, D.; Fiorani, F.; Rascher, U.; Schneider, H.U.; Walter, A.; Schurr, U. Non-invasive phenotyping methodologies enable the accurate characterization of growth and performance of shoots and roots. In *Genomics of Plant Genetic Resources*; Tuberosa, R., Graner, A., Frison, E., Eds.; Springer: Dordrecht, The Netherlands, 2014; pp. 173–206.
5. Rascher, U.; Blossfeld, S.; Fiorani, F.; Jahnke, S.; Jansen, M.; Kuhn, A.J.; Matsubara, S.; Martin, L.L.A.; Merchant, A.; Metzner, R.; *et al.* Non-invasive approaches for phenotyping of enhanced performance traits in bean. *Funct. Plant Biol.* **2011**, *38*, 968–983.
6. Hillnhütter, C.; Mahlein, A.-K. Neue ansätze zur frühzeitigen erkennung und lokalisierung von zuckerrübenkrankheiten. *Gesunde Pflanzen* **2008**, *60*, 143–149.
7. West, J.S.; Bravo, C.; Oberti, R.; Lemaire, D.; Moshou, D.; McCartney, H.A. The potential of optical canopy measurement for targeted control of field crop diseases. *Annu. Rev. Phytopathol.* **2003**, *41*, 593–614.
8. Rascher, U.; Agati, G.; Alonso, L.; Cecchi, G.; Champagne, S.; Colombo, R.; Damm, A.; Daumard, F.; de Miguel, E.; Fernandez, G.; *et al.* Cefles2: The remote sensing component to quantify photosynthetic efficiency from the leaf to the region by measuring sun-induced fluorescence in the oxygen absorption bands. *Biogeosciences* **2009**, *6*, 1181–1198.
9. Buschmann, C.; Nagel, E. *In vivo* spectroscopy and internal optics of leaves as basis for remote-sensing of vegetation. *Int. J. Remote Sens.* **1993**, *14*, 711–722.
10. Gamon, J.A.; Surfus, J.S. Assessing leaf pigment content and activity with a reflectometer. *New Phytol.* **1999**, *143*, 105–117.
11. Bock, C.H.; Poole, G.H.; Parker, P.E.; Gottwald, T.R. Plant disease severity estimated visually, by digital photography and image analysis, and by hyperspectral imaging. *Crit. Rev. Plant Sci.* **2010**, *29*, 59–107.
12. Huete, A.R. A soil-adjusted vegetation index (SAVI). *Remote Sens. Environ.* **1988**, *25*, 295–309.
13. Mahlein, A.K.; Rumpf, T.; Welke, P.; Dehne, H.W.; Plümer, L.; Steiner, U.; Oerke, E.C. Development of spectral indices for detecting and identifying plant diseases. *Remote Sens. Environ.* **2013**, *128*, 21–30.
14. Rouse, J.W.; Haas, R.H.; Schell, J.A.; Deering, D.W. Monitoring vegetation systems in the great plains with ERTS. In *Proceedings of the Third ERTS Symposium*; NASA SP-351; NASA: Washington, DC, USA, 1973; pp. 309–317.
15. Gamon, J.A.; Peñuelas, J.; Field, C.B. A narrow-waveband spectral index that tracks diurnal changes in photosynthetic efficiency. *Remote Sens. Environ.* **1992**, *41*, 35–44.
16. Penuelas, J.; Baret, F.; Filella, I. Semiempirical indexes to assess carotenoids chlorophyll-a ratio from leaf spectral reflectance. *Photosynthetica* **1995**, *31*, 221–230.
17. Blackburn, G.A. Spectral indices for estimating photosynthetic pigment concentrations: A test using senescent tree leaves. *Int. J. Remote Sens.* **1998**, *19*, 657–675.

18. Peñuelas, J.; Piñol, J.; Ogaya, R.; Filella, I. Estimation of plant water concentration by the reflectance water index WI (R900/R970). *Int. J. Remote Sens.* **1997**, *18*, 2869–2875.
19. Gitelson, A.A.; Zur, Y.; Chivkunova, O.B.; Merzlyak, M.N. Assessing carotenoid content in plant leaves with reflectance spectroscopy. *Photochem. Photobiol.* **2002**, *75*, 272–281.
20. Gitelson, A.A.; Merzlyak, M.N.; Chivkunova, O.B. Optical properties and nondestructive estimation of anthocyanin content in plant leaves. *Photochem. Photobiol.* **2001**, *74*, 38–45.
21. Gao, B.-C. Ndw—A normalized difference water index for remote sensing of vegetation liquid water from space. *Remote Sens. Environ.* **1996**, *58*, 257–266.
22. Chen, D.; Huang, J.; Jackson, T.J. Vegetation water content estimation for corn and soybeans using spectral indices derived from modis near- and short-wave infrared bands. *Remote Sens. Environ.* **2005**, *98*, 225–236.
23. Seelig, H.-D.; Hoehn, A.; Stodieck, L.S.; Klaus, D.M.; Emery, W.J.; Adams, W.W., III. Relations of remote sensing leaf water indices to leaf water thickness in cowpea, bean, and sugarbeet plants. *Remote Sens. Environ.* **2008**, *112*, 445–455.
24. Weiland, J.; Koch, G. Sugarbeet leaf spot disease (*Cercospora beticola* Sacc.). *Mol. Plant Pathol.* **2004**, *5*, 157–166.
25. Rumpf, T.; Mahlein, A.K.; Steiner, U.; Oerke, E.C.; Dehne, H.W.; Pluemer, L. Early detection and classification of plant diseases with support vector machines based on hyperspectral reflectance. *Comput. Electron. Agric.* **2010**, *74*, 91–99.
26. Mahlein, A.K.; Steiner, U.; Dehne, H.W.; Oerke, E.C. Spectral signatures of sugar beet leaves for the detection and differentiation of diseases. *Precis. Agric.* **2010**, *11*, 413–431.